Analysis of the mechanical loading and failure of tendons

BME 530 Final Project

Jason Liu and Callan Corcoran

18 April 2016

Introduction

The muscle-tendon unit (MTU) is responsible for human movement. Muscle is a soft tissue, consisting of cells with highly aligned contractile elements known as sarcomeres, which exert tensile forces that change the tissue's length and shape. This tensile force is transferred through muscle epimysium, through tendon, through the periosteum layer, to surrounding bones. This chain of connections allows for muscle contractions to translate into skeletal motion.

Damage to any part of this chain can lead to pain, moderate impairment of motion, or even complete impairment of motion. Tendon often represents the weak link in this chain, because the tissue transmits high tensile loads and must store and release energy during motion. Furthermore, tendon tissue has low cell density and is not significantly vascularized, so repair mechanisms are limited and slow. Repairs of ruptured tendons more often rely on surgical placement of high-tensile-strength sutures rather than letting the human body naturally repair the rupture. Because tendon damage can lead to impairment of motion and pain without surgical intervention, further investigation of tendon damage pathology is invaluable.

Short term tendon damage, or tendonitis, is not completely understood, partly because the because there is no way of clearly observing even normal tendon mechanics *in situ*. There are several studies that have sought to explain healthy tendon mechanics through discrete-element viscoelastic models (Roux et al., 2016), and recent studies have used ultrasound and load cells to model Achilles tendon deformation and loading to characterize the in-vivo passive mechanical properties of tendon (de Oliviera et al., 2015). There has not been a mechanical model for damaged tendon, which is what we seek to do in this study.

Methods

The model for damaged human tendon is based on mechanical fatigue models of rat patellar tendon in Fung et al. (2009), with mechanical coefficients defined in de Oliviera et al. (2015). This general model is then applied with elastic modulus values for collagen components derived from Wagner et al. (2007) and Dutov et al. (2015). A comparison of model results to the literature value for collagen ultimate strain (Shen et al., 2008) helps to determine the point of failure for muscle tendons.

Modeling mechanics of tendon

To start, the physiology of tendon was explored and outlined. Tendon is made up overlapping and aligned collagen molecules on several orders of organization, as shown in Appendix Figure 3. There are individual collagen I molecules, which are woven together into fibrils, which are placed together in fascicles, which are bundled into full tendons. Appendix Figure 3 show the very anisotropic, uniaxially aligned collagen that make up the full tendon. Because of the strong tensile properties of collagen, the high level of orientation and organization accentuate these uniaxial tensile properties at a macroscopic scale. To complete the physiological characterization of tendon, between these aligned fibrils are tenocytes, cells that regulate the tendon environment. Given this, we modeled (assumed) tendon as many strands of aligned collagen fibrils in parallel, taking into consideration the true mechanics of tendon in ex-vivo experiments with

tendon. We ignored the tensile strength of the tenocytes and assumed the mechanical loading of the tendon was conducted faster than the tenocytes could respond and attempt to repair collagen fiber rupture.

The rat patellar tendon model in Fung et al. showed multiphoton microscopy images of tendon collagen matrices after tensile loading. At low loads, the matrix seemed very un-damaged and maintained, but at high loads, the matrix was severely disrupted and many discontinuities in the matrix could be seen. The study concluded that there was an observable increase in stiffness with higher strains which the authors attributed to fiber recruitment that redistributes loads from damaged to undamaged fibers during cyclic loading. Even higher levels of deformation and strain lead to a reduction in stiffness (Fung et al., 2008).

We interpreted this as two competing forces at play when straining tendon: an increase in stiffness due to recruitment of strands at moderate levels of strain, and decrease in stiffness due to the breakage of strands at high levels of strain. In order to model this, we varied the lengths of the strands of collagen in our model, which meant that at a specific deformation state length, only strands of collagen with lengths smaller than that deformation length were "recruited," or strained, and thus were the only strands able to exert a force and stress. We also set an ultimate strain value at which the collagen strands would break if their strain would exceed this value. These two conditions modeled these two competing forces.

The following sections outline the process in estimating elastic modulus of these collagen strands, which will give insight into the stiffness of the strands. Additionally, we discuss the mathematical theory underpinning the model.

Estimating the elastic modulus of collagen fibers

Much effort has been devoted to identifying the elastic modulus of collagen fibers, both as individual strands and bundled in collagen fibrils. Across studies, researchers have found that there are significant discrepancies in observed elastic moduli that are largely dependent upon dehydration of the samples, variation across individual samples, and the susceptibility of AFM cantilevers (commonly used to identify material properties of molecules) to inaccurate measurement (Wenger 2007) (Dutov 2015). Some researchers have even leveraged this highly variable property, seeking to tune the elastic modulus of collagen samples (Grant 2009).

In this study, we elect to leverage the findings of Dutov et al., which relate elastic modulus of collagen fibers to the radius of the fibrils (2015). The researchers identify an average elastic modulus (E_{avg}) that varies with hydration, and is grounded largely in the literature (Table I). This estimated average modulus can then be compared to a plot of $(E^*R^4/E_{avg})^{¼}$ to identify the individual elastic modulus for a collagen fibril of a given radius (Figure 1).

In tandem with the findings of Dutov and Wenger, we have opted to estimate the properties of a collagen fibril with a radius of 180 nm (or diameter of 360 nm). This represents roughly the 90th percentile of cumulative probability per Dutov et al., and is in keeping with estimates of fibril properties outlined by Shoulders et al. (2009). Given that the maximum length of individual collagen fibers is estimated to be 1 cm

(Shoulders 2009), we chose to model a unit of collagen fibers in parallel with an average length of 0.9 cm, or 90% of the maximum length. We selected an E_{avg} value that approximated 30% relative humidity (see Table I), and thus set it at E_{avg}=14.7 GPa (Wenger 2007). Depending on the conditions of interest, these assumptions can be changed in our model through an alteration of the MATLAB code (see Appendix).

Given these parameters, the graph given by Dutov et al. (2015) can be used to derive E for the collagen fibril of interest, noting that the slope at the radius of interest is equal to $(E/E_{avg})^{¼}$. Dutov's plot indicates the slope of this relationship varying for different fibril radii; for the region of interest in our analysis, this slope is estimated to be 5.36. Thus, the estimated elastic modulus for our model is 10.51 GPa.

Ultimate strain of collagen fibers

As changing conditions are wont to alter the elastic modulus of collagen, so too do differences in hydration alter ultimate strain. Shen et al. have examined the highly variable properties of individual collagen properties, which can withstand strain of over 100% in some conditions, and exhibit ultimate strain as low as 5% following embrittlement via dehydration (2008). For our model we opted for a moderate estimate of ultimate strain, and chose to use Shen et al.'s observed 13% ultimate strain for conditions of initial dehydration and re-hydration prior to testing, which we believe best model our chosen conditions of 30% relative humidity.

Modeling tendons as collagen fibers in parallel

The goal of our model is to recreate the stress strain curve often found in tensile-loaded tendon samples. Given that collagen is the major component of tendon that contributes to tensile strength (tenocytes resist some stresses, but collagen is many order of magnitudes higher in both elastic modulus and ultimate stress), we model tendon as only collagen. Specifically, we model loading of tendon as many strands of collagen as cylindrical beams in parallel, loaded uniaxially in a fashion similar to simple extension. Following Section 5.13 in the Lai et al. text (2010), the fibrils of collagen are cylindrical bars under the action of equal and opposite normal traction stress distributed uniformly at the two end-faces, with no surface tractions on the lateral surface and there are no body forces. Figure 2 illustrates one such cylinder, which is a component of the hierarchical muscle structure depicted in Figure 3.

The first step in this model is establishing the geometry of the tendon model. The number of strands dictates the cross section of the tendon model, using the following equation:

$$total\ cross\ sectional\ area = \pi \times \left(\frac{diameter\ of\ one\ cylindrical\ beam}{2}\right)^2 \times number\ of\ strands$$

The length of the model as discussed above will have a set initial length, and when axial loading occurs, there will be axial and transverse deformation. The overall deformation is dictated by Hooke's law:

$$E_{11} = \frac{1}{E_Y}\left[T_{11} - v(T_{22} + T_{33})\right] = \frac{T_{11}}{E_Y};$$

$$E_{22} = \frac{1}{E_Y}\left[T_{22} - v(T_{33} + T_{11})\right] = E_{33}$$

Where E_{11} is the axial deformation, σ is the axial stress, T_{11},T_{22},T_{33} are the stresses in the axial, transverse, and transverse directions, respectively, and v is Poisson's Ratio.

Poisson's ratio is defined as the following:

$$v = -\frac{E_{transverse}}{E_{axial}}$$

Where E is the deformation as defined above

The boundary conditions to this simple extension model match as follows:

$$T_{11} = \sigma, \quad T_{22} = T_{23} = T_{12} = T_{13} = T_{33} = 0$$

The equations of equilibrium are satisfied given these conditions because all stress components are either constant or zero and the equations of equilibrium are satisfied assuming no body forces exist. There are three boundary surfaces, and the boundary conditions are satisfied for the two axial ends. On the lateral surface, the unit outward normal does not have an axial component.

The MATLAB code was set up such that the model can take any elastic modulus, Poisson ratio, any variation of collagen length, number of strands of collagen, overall strain, diameters of the cylindrical models of collagen, and the maximum strain at which collagen fibers begin to break. We used values that we believed to be around average for a 1 cm long tendon; which are listed within the MATLAB code in the appendix. The code iterated through a set number of possible strains of the overall tendon model, through every single cylinder included in the model, to determine whether the cylinder was recruited at that strain level, the cylinder's equivalent stress given that strain, and checked if that cylinder "breaks" at that strain level. For each strain level, the sum of the stress for all recruited cylinders determined the total stress of the entire tendon.

Results

We modeled (assumed) tendon as many strands of aligned collagen fibrils in parallel. We took each fibril as a thin cylinder under simple extension along the long axis. We ignored the tensile strength of the tenocytes and assumed the mechanical loading of the tendon was conducted faster than the tenocytes could respond and attempt to repair collagen fiber rupture. We varied the lengths of the cylinders in our model, which meant that at a specific deformation state length, only cylinders with lengths smaller than that deformation length were "recruited," or strained, and thus were the only cylinders able to exert a force and stress. We also set an ultimate strain value at which the cylinders would not exert a stress if their strain would exceed this value. The use of the above equations in the methods section assumes that the cylinders are isotropic linearly elastic solids. For the purposes of this simulation, because it is simple extension, this assumption can be used.

The results of the model reflect the mechanics of actual tendon as demonstrated in the stress-strain curve shown in Figure 4. Given the best estimate values for the geometry and mechanical constants of the tendon, we achieved the components of the stress/strain characteristics of tendon that we sought to acquire in our methods-- successfully displaying the increased stiffness of the tendon at moderate

strains, and “breaking” of strands at high strains. The “bumpy” plateau at high strain appears, showing this competing effect between breaking shorter strands while recruiting longer strands. This matches the stress strain curve of tendon in several previous studies At around 0.2 strain, the amount of stress in the model drops off sharply, as the majority of collagens are broken and continue to break.

We found that the ultimate strain value strongly dictated the location where the strain-stiffening properties of the model would level off. We found that strain stiffening to be roughly parabolic, because our model linearly varied the lengths of the cylinders, so the loading should roughly fit a positively-inflected second-order function. The plateau region’s shape was very exciting to observe as it starts very abruptly (similar to the quick rupture of tendon that occurs in-vivo) and holds a stress to a wavering amount, and then drops off similarly to a negatively-inflected second-order function.

A mathematical solution to our model could not be reasonably obtained because the analysis requires the computation of several million strain and stress calculations for each thin cylinder at all strains.

Discussion

It is difficult to estimate the scope of tendon injuries worldwide, as many go untreated and the genesis of the injuries varies greatly. Though the majority of these injuries are thought to be sustained by athletes, those with a sedentary lifestyle are at high risk for injury as well (Kvist, 1994). A study by Clayton et al. in the Royal Infirmary of Edinburgh indicated that roughly 167/100,000 males and 52/100,000 females in the area sustained musculoskeletal injuries each year (2008). Hand tendon injuries and Achilles’ tendon tears are among the most common injuries observed. The researchers also demonstrated that the incidence of many of these injuries increases with age. These data make clear that the failure of tendons is of clinical importance, as it is a commonly observed injury, and that the changing properties of collagen (such as its dehydration and embrittlement with age) are critical factors in understanding the mechanism of failure.

Our model provides a flexible platform upon which tendon failure can be better studied and understood, accounting for factors that dramatically alter the material properties of the collagen fibers that compose the tendon. We chose to examine a specific set of tendon conditions as a proof of concept, but in the future this model may prove valuable in simulating changing conditions with age or exercise. With this model in mind, it may be possible to identify those at risk of tendon failure and accordingly minimize risk of reaching the tendon’s ultimate strain. The model put forth here could also herald the development of wearable medical devices to monitor tendon exposure to strain, potentially warning those at risk when they are entering a range of exercise that puts them at risk for injury.

The model has some weaknesses inherent in its assumptions about the properties of individual collagen fibers; for a general case, it is hard to assert that these selected parameters are accurate. However, the flexibility of the MATLAB code in altering these initial conditions opens up great possibility in tailoring the model to individual cases. Our code assumes a very quick strain rate such that the body cannot biologically react to the mechanical loading. In reality, tendons undergo cyclic straining and many other factors contribute to tendon mechanical failure. Further development of tendon models could be developed,

and more factors can be accounted for in tendon damage such as longer time scale, cyclic-fatigue damage, permanent deformation of collagen, the mechanical properties of tenocytes and their biological response to not only strain but also shear and von Mises stress.

References

Clayton, RAE, and Court-Brown, CM. "The epidemiology of musculoskeletal tendinous and ligamentous injuries." *International Journal of the Care of the Injured*, Vol 39: 1338-1344. 30 June 2008. Web.

de Oliviera, LF, Peixinho, CC, Silva, GA, and Menegaldo, LL. "*In vivo* passive mechanical properties estimation of Achilles' tendon using ultrasound." *Journal of Biomechanics*, Vol 49(4): 507-513. 29 February 2016. Web.

Dutov, P, Antipova, O, Varma, S, Orgel, JPRO, and Schieber, JD. "Measurement of Elastic Modulus of Collagen Type I Single Fiber." *PLoS One*, Vol 11(1). 22 January 2016. Web.

Fung, DT, Wang, VM, Andarawis-Puri, N, Basta-Pljakic, J, Li, Y, Laudier, DM, Sun, HB, Jepsen, KJ, Schaffler, MB, and Flatow, EL. "Early response to tendon fatigue damage accumulation in a novel in vivo model." *Journal of Biomechanics*, Vol 43(2): 274-279. 25 August 2009. Web.

Grant, CA, Brockwell, DJ, Radford, SE, and Thomson, NH. "Tuning the Elastic Modulus of Hydrated Collagen Fibrils." *Biophysical Journal*, Vol 97: 2985-2992. 3 September 2009. Web.

Kondratko-Mittnacht, J, Lakes, R, and Vanderby, R. "Shear loads induce cellular damage in tendon fascicles." *Journal of Biomechanics*, Vol 48(12): 3299-3305. 18 September 2015. Web.

Kvist, M. "Achilles tendon injuries in athletes." *Sports Medicine*, Vol 18(3): 173-201. 1994. Web.

Lai, WM, Rubin, D, and Krempl, E. *Introduction to Continuum Mechanics*, Fourth Edition. Elsevier, 2010.

Neviaser, A, Andarawis-Puri, N, and Flatow, E, "Basic mechanisms of tendon fatigue damage." *Journal of Shoulder and Elbow Surgery*, Vol 21(2): 158-163. February 2012. Web.

Roux, A, Laporte, S, Lecompte, J, Gras, LL, and Jordanoff, I. "Influence of muscle-tendon complex geometrical parameters on modeling passive stretch behavior with the Discrete Element Method." *Journal of Biomechanics*, Vol 49(2): 252-258. 3 December 2015. Web.

Shen, ZL, Dodge, MR, Kahn, H, Ballarini, R, and Eppell, SJ. "Stress-Strain Experiments on Individual Collagen Fibrils." *Biophysical Journal*, Vol 95: 3956-3963. October 2008. Web.

Shoulder, MD, and Raines, RT. "Collagen structure and stability." *Annual Review of Biochemistry*, Vol 78: 929-958. 2009. Web.

Vergari, C, Pourcelot, P, Holden, L, Ravary-Plumioen, B, Gerard, G, Laugier, P, Mitton, D, and Crevier-Denoix, N. "True stress and Poisson's ratio of tendons during loading." *Journal of Biomechanics*, Vol 44(4): 719-724. 24 February 2011. Web.

Wenger, MPE, Bozec, L, Horton, MA, and Mesquida, P. "Mechanical Properties of Collagen Fibrils." *Biophysical Journal*, Vol 43: 1255-1293. 7 April 2007. Web.

Appendix

Table I. Wenger et al. compilation of observed Young's moduli for tendons across various studies and conditions (2007). Young's moduli vary significantly with quantification technique and state of fibril.

TABLE 1 Young's modulus of collagen

Collagen fibril (Ref.)	Technique	State of fibril	Young's mod. (GPa)
Rat tail tendon*	Indentation	Different dehydration states	3.75–11.5
Rat tail tendon (34)	Brillouin	In 0.15 M NaCl solution	9.0
Rat tail tendon (34)	Brillouin	At 30% relative humidity	14.7
Rat tail tendon (34)	Brillouin	At 0% relative humidity	21.5
Rat tail tendon (35)	Brillouin	In 0.15 M NaCl solution	5.1
Rat tail tendon (35)	Brillouin	At 50% relative humidity	11.9
Bovine Achilles tendon (36)	X ray	In 0.15 M NaCl solution	2.9 ± 0.1
Bovine Achilles tendon (17)	Spectroscopy	At 0% relative humidity	2–7
Bovine Achilles tendon (17)	Spectroscopy	In phosphate buffered saline	0.2–0.5
Sea cucumber (13)	Tensile test	In water	12 (high strain)
Sea cucumber (24)	Indentation	<45% relative humidity	1–2
Collagen-like peptide (37)	Simulation	—	4.8 ± 1.0

Note: Harley et al. (34) and Cusack and Miller (35) are spectroscopic measurements performed at hyper-sound frequencies in the GHz range.
*Present work.

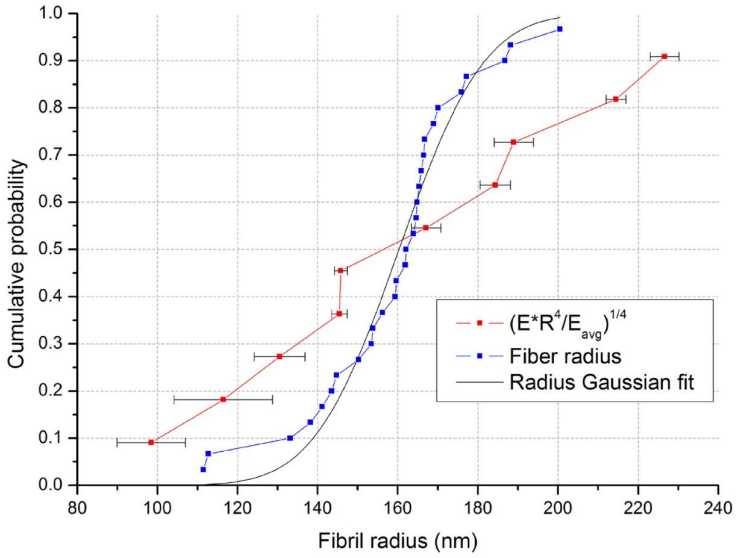

Figure 1. Dutov et al.'s relation of elastic modulus, fiber radius, and average elastic modulus (based upon conditions such as hydration) (2015). In blue is the cumulative distribution of the fiber radius, and in black is the Gaussian fit for this distribution. In red are values for $(E^*R^4/E_{avg})^{¼}$, used to relate the value of E_{avg}, determined from experimental estimates of elastic modulus, and the elastic modulus (E) of an individual fiber with radius R.

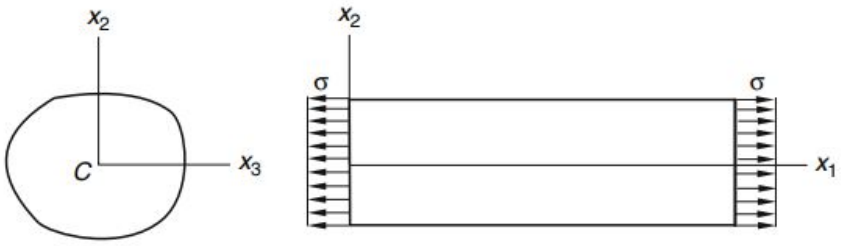

Figure 2: Diagram of a cylinder under simple extension. On the left is a general cross sectional area, and the right is a rough sketch of the stresses on the body. Our tendon model seeks to employ this model, but extend it by having many cylinders of collagen in parallel.

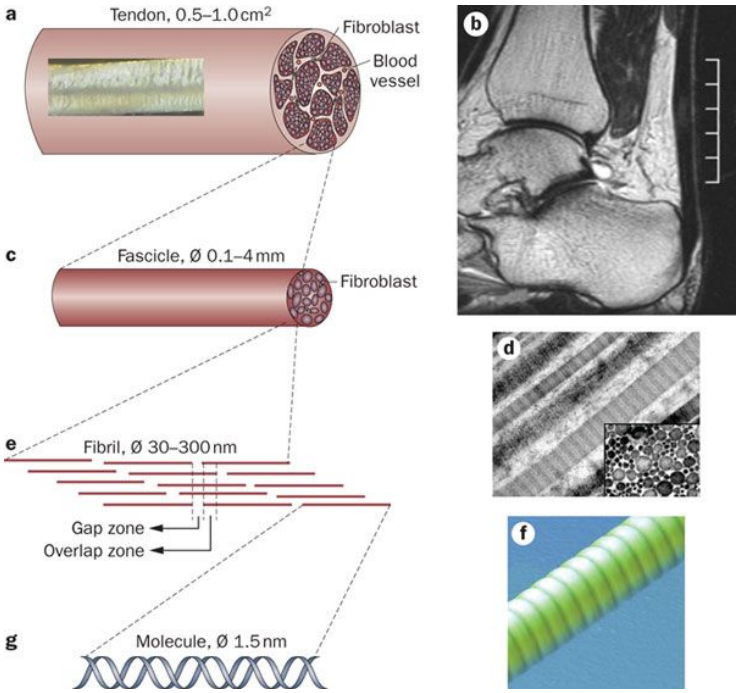

Figure 3. Diagram of the hierarchical structure of muscle tendon, which is comprised of fascicles, in turn comprised of fibroblasts, which are made of overlapping fibrils. Fibrils are bundles of collagen molecules.

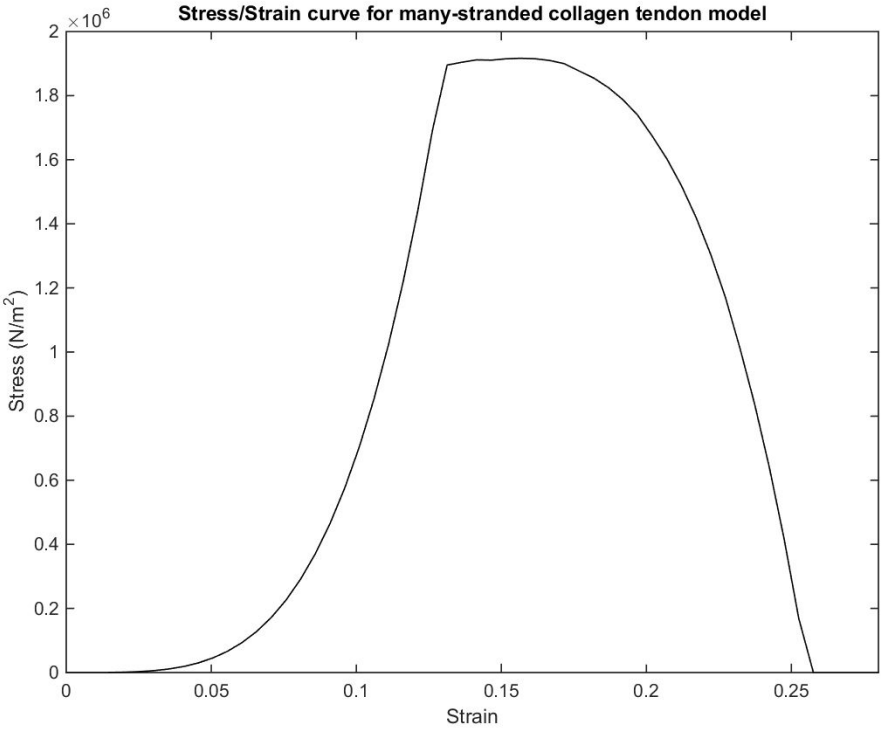

Figure 4: Stress strain curve for the many-collagen-strands tendon model. Note the strain-stiffening that occurs at around 0.05 strain, where more strands of collagen are recruited and thus the effective cross sectional area and stiffness of the tendon increases, so stress increases at an exponential rate. When strain hits approximately 0.13, the fibers begin to "break", and a "bumpy" plateau appears, showing a competing effect between breaking shorter strands while recruiting longer strands. At around 0.2 strain, the amount of stress in the model drops off sharply, as the majority of collagens are broken and continue to break.

Code A. MATLAB code used in mathematical analysis.

```
%% this is a tendon model collagen as many strands as thin cylinders
clear all;

elastic_Modulus=10.51*(10^9); % in N/m2
poisson_ratio= -0.55; % according to Vergari in 2010

smallest_length=0.009; % smallest length of collagen in m
largest_length=0.01; % largest length of collagen in m
variation_ratio=0.10; % percent of variation in the length to model strain
recruitment
strand_number=1000; % total number of strands of collagen
end_displacement=linspace(0,0.5,100); % make an array for strain, from 0 to 0.5
strain
initial_diameter=180*(10^-9); % average diameter is 180 nm
strand_lengths=linspace(smallest_length,largest_length,strand_number);
max_strain=0.13; % strain as defined in Shen et al.
employed_strand_array=zeros(1,strand_number); % keeps track of which strands
are employed
strain=zeros(1,strand_number);
```

```
stress=zeros(1,strand_number);
force_exerted_each_strand=zeros(1,strand_number);
CSA=zeros(1,strand_number);
break_array=zeros(1,strand_number); % keeps track of which strands have broken.
% the strand length will vary linearly between the minimum and maximum lengths
given
initial_end_position=0.009;

cross_sectional_area=@(diameter,strands) pi.*((diameter./2).^2)*strands;
stress_func=@(strains) elastic_Modulus.*strains;
transverse_strain=@(strains2) -1.*poisson_ratio.*strains2;

    disper_iteration=1;

for disp_iteration=end_displacement % iterating through every possible strain
from 0 to 0.5
    for strand_iteration=1:strand_number % iterating through every strand
        % checking if the strand is employed. if the length of the strand
        % is smaller than that of the position of the end, then it is
        % effectively employed and the end will be strained to that position.
        if
strand_lengths(strand_iteration)<=(initial_end_position+(disp_iteration*initial
_end_position))
            employed_strand_array(strand_iteration)=1;
        end
        if employed_strand_array(strand_iteration) % if is strained, the strain
of that strand
            % is calculated by finding the difference in end position and
            % the initial length of the strand and dividing by the original
            % length of the strand.

strain(strand_iteration)=(initial_end_position+(initial_end_position*disp_itera
tion)-strand_lengths(strand_iteration))/strand_lengths(strand_iteration);
%calculating the strain of each strand
            % stress is just the elastic modulus times the strain.
            stress(strand_iteration)=stress_func(strain(strand_iteration));

            if strain(strand_iteration)>0.13 %if strain of a strand is greater
than the maximum strain, the strand is "broken" and can no longer hold stress.
                stress(strand_iteration)=0;
                break_array(strand_iteration)=1;
            end
            % as the strands are strained in the axial direction, there
            % will be strain in the transverse according to poisson's
            % ratio.

new_diameter=transverse_strain(strain(strand_iteration)).*initial_diameter;
            CSA(strand_iteration)=cross_sectional_area(new_diameter,1);

force_exerted_each_strand(strand_iteration)=stress(strand_iteration).*CSA(stran
d_iteration);
        end
    end
    force_total(disper_iteration)=sum(force_exerted_each_strand);
```

```
    disper_iteration=disper_iteration+1;
end

figure(1)
stress_total=force_total./cross_sectional_area(initial_diameter,strand_number);
plot(end_displacement,stress_total,'k-');
title('Stress/Strain curve for many-stranded collagen tendon model');
xlabel('Strain');
ylabel('Stress (N/m^2)');
axis([0 0.28 -inf 20*10^5]);
print('stress_strain_tendon','-dpng');
```